EPSC Abstracts
Vol. 7 EPSC2012-751 2012
European Planetary Science Congress 2012

Long-wavelength topographic change in the Caloris basin, Mercury

Christian Klimczak (1), Paul K. Byrne (1), Sean C. Solomon (1), Carolyn M. Ernst (2), and Thomas R. Watters (3)

(1) Department of Terrestrial Magnetism, Carnegie Institution of Washington, Washington DC 20015, USA (cklimczak@ciw.edu); (2) The Johns Hopkins University Applied Physics Laboratory, Laurel, MD 20723, USA; (3) Center for Earth and Planetary Studies, National Air and Space Museum, Smithsonian Institution, Washington, DC 20560, USA.

1. Structure of the Caloris basin

The 1550-km-diameter Caloris basin is the largest preserved impact basin and the most geologically complex tectonic province on Mercury. Data returned by the MESSENGER spacecraft reveal a rich history of volcanic and tectonic activity in Caloris, as well as post-impact changes to the long-wavelength topography of the basin floor. In particular, smooth volcanic plains deposits that partially fill the basin [1] were affected by extensional as well as contractional deformation [2], evident by the juxtaposition of normal- and thrust-fault-related landforms, such as graben and wrinkle ridges. Both graben and wrinkle ridges are found in orientations radial and circumferential to the basin as well as in unoriented arrays [3, 4]. Apart from a few wide graben that cut narrower graben in the basin center [5], cross-cutting relationships yielding conclusive relative age relations between landforms have not been reported on.

Moreover, both altimetry profiles [6] and stereo-derived terrain models [7] reveal that the basin floor experienced long-wavelength topographic change subsequent to interior plains emplacement. Portions of the floor are now more elevated than the basin rim [6] and floors of many interior impact craters tilt away from the elevated areas [6, 8]. The anomalous topography does not correlate with the distribution or orientations of tectonic landforms within the basin [7]. No combination of tectonic processes has yet been found that can account both for the topography and for the types and orientations of tectonic landforms in the Caloris basin.

2. Objective

We use information on (*1*) depths of faulting inferred from graben geometry [9] and (*2*) depth of excavation of spectrally distinct geological units from impact cratering [10] to infer the thickness of the uppermost layer of smooth plains in the Caloris basin. We then correlate layer thickness with topography to obtain insights into the style, mechanism, and timing of long-wavelength topographic change within the basin.

3. Plains thickness

Among the many graben in the Caloris interior plains (Fig. 1), radial graben in the central part of the basin as part of Pantheon Fossae are best suited for fault geometric analysis. Geometrical fault properties, such as lengths and displacements, can be utilized to infer the depth of faulting associated with the graben. Fault displacement profiles and displacement-to-length scaling of the faults both reveal that there are restricted and unrestricted faults [9]. Restricted faults are confined to a mechanical unit that extends to 2.7 to 4 km depth and are located mainly in the central part of Caloris, whereas unrestricted faults, which are found farther from the basin center, extend as deep as 8 km [9].

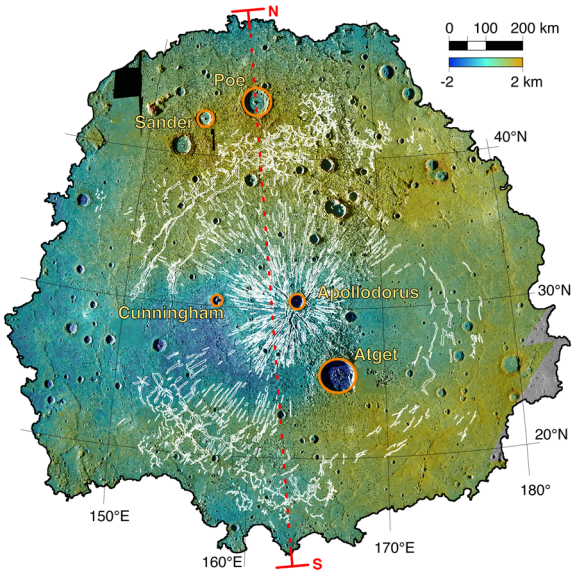

Figure 1. MESSENGER image mosaic of the Caloris basin with overlaid topography and prominent graben (white). The red line indicates the location of the profile in Fig. 2.

The established displacement-to-length scaling relationship can be used to infer the maximum depth of faulting for every normal fault in Caloris, if either length or maximum displacement of the fault is known. A set of >150 faults, distributed throughout the Caloris basin, was used to compute a map of depth extent of faulting [9]. Where faults are restricted, this depth marks a boundary between mechanical units.

4. Origin of topographic change

The basin topography is characterized by two elongate high-standing areas in the northern and southern parts of the basin, separated by an elongate topographic low with its deepest point just southwest of the basin center (Fig. 1). A topographic profile from north to south through the central region of Caloris (Fig. 2) illustrates that the long-wavelength topography can be described as nearly harmonic folding. The folds have

a wavelength of ~1200 km and a peak-to-peak amplitude of ~2.5 km.

Relating the topography to the depth extent of faulting (Fig. 2) shows that graben grew deeper in areas of high-standing topography, whereas the restricted graben in the topographically lower parts of the Caloris basin have shallower depth extents of faulting. These co-variations indicate substantial variations in the thickness of the uppermost unit, identified here with the interior smooth plains material. Excavation of spectrally differing units [10] from five nearby impact craters (Fig. 1) are consistent with the depth extents of faulting and the thickness changes sketched in Fig. 2. This agreement suggests that the change of spectral properties at depth beneath the Caloris smooth plains coincides with the base of the mechanical layer in which the faults grew.

The variations in the thickness of the smooth plains material include a greater thickness at high-standing areas and a lesser thickness at topographic lows, suggesting a large-scale pinch-and-swell geometry of the layer (Fig. 2). A scenario that accounts for this structure involves continuous lithospheric folding and episodic plains emplacement (Fig. 3). In particular, after basin formation and an initial episode of volcanism leading to the emplacement of volcanic plains on the basin floor (Fig. 3a, left), folding modified the basin topography by introducing a topographic high in the center and lows on the north and south portions of the basin floor (Fig. 3b, left). Further volcanism led to the emplacement of smooth plains units that pooled in the low areas and partially flooded the higher areas, introducing changes in layer thickness (Fig. 3c, left). Continuing lithospheric folding then led to pinching of the uppermost mechanical unit at the thinner parts of the unit and a swelling in the thicker parts of the unit (Fig. 3d, left), producing the present-day topography (Figs. 1, 2). This scenario, however, does not account for the second set of younger and wider graben in the center of Pantheon Fosse that are suggested to have greater depth extents of faulting [5]. This omission can be treated by introducing a multi-ring geometry for the initial Caloris basin profile, one in which the central parts of the basin floor were topographically lower than the outer portions (Fig. 3a-d, right).

Long-wavelength topographic change was a global process on Mercury, as there is evidence for folding outside the Caloris basin and elsewhere on the planet [6, 8, 11]. In contrast, the graben and wrinkle ridges within the Caloris interior plains are products of basin-specific tectonics and were apparently unaffected by the changes to long-wavelength topography (Fig. 1). This lack of correlation is consistent with the low strain accommodated by the lithospheric folds (strain ~ 10^{-5}). We infer that stresses during folding were minor to have large effects on the orientations of later-formed graben and wrinkle ridges.

References

[1] S. L. Murchie et al., Science, 321, 73, 2008.
[2] T. R. Watters et al., Earth Planet. Sci. Lett., 285, 309, 2009.
[3] P. K. Byrne, Lunar Planet. Sci., 43, 1722, 2012.
[4] P. K. Byrne et al., EPSC, 2012, this mtg.
[5] C. Klimczak et al., Icarus, 209, 262, 2010.
[6] M. T. Zuber et al., Science, 336, 217, 2012.
[7] J. Oberst et al., Icarus, 209, 230, 2010.
[8] J. A. Balcerski et al., Lunar Planet. Sci., 43, 1850, 2012.
[9] C. Klimczak et al., Lunar Planet. Sci., 43, 1959, 2012.
[10] C. M. Ernst et al., 209, 210, Icarus, 2010.
[11] S. C. Solomon et al., Lunar Planet. Sci., 43, 1578, 2012.

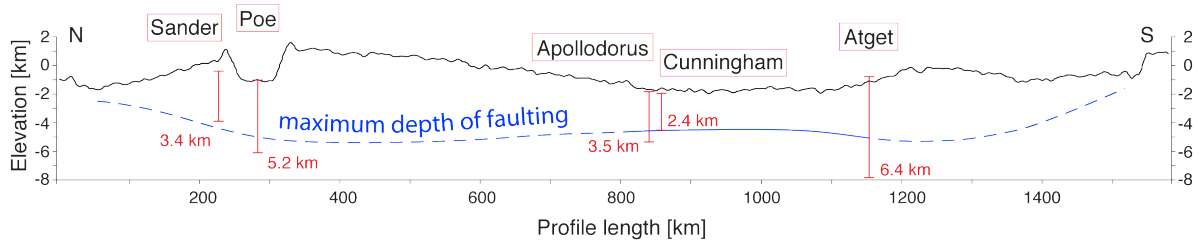

Figure 2. Topographic profile from north to south across the Caloris basin showing inferred depth extent of faulting [8] and depths of excavation of material that is spectrally distinct from the surface plains material [9].

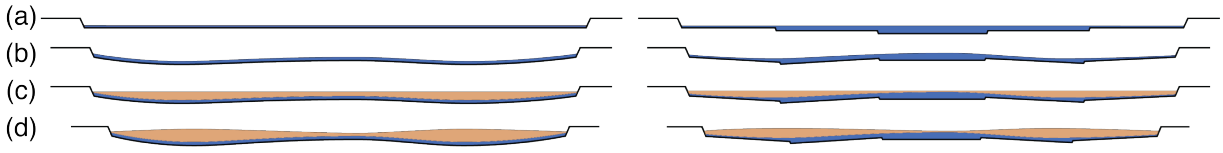

Figure 3. Schematic depiction of the development of long-wavelength topography in the Caloris basin by continuing folding and episodic plains emplacement. Left-hand column depicts scenario with simple basin floor geometry, whereas right-hand column shows a multi-ring geometry.